Chapter 5

Experimental Results

5.1 Instrument and Experiment Flow

All the experiments were applied by the camera, Nikon D70, with “exposure bracket” mode. The scenes with high and low luminance were chosen for our HDR application. The experiment flow is shown in **Fig. 5-1**. The camera response curve is firstly estimated on computer by collecting images with different scenes and the weighting function is achieved later. Then inserting both of them into the specific camera is to be the data base. Two images with high and low exposures are taken by this camera and the low one is shifted by our image registration algorithm. The shifted and fixed images are then fused by our image fusion algorithm. After color and edge enhancement of the fused image, the HDR image will be output to the camera.

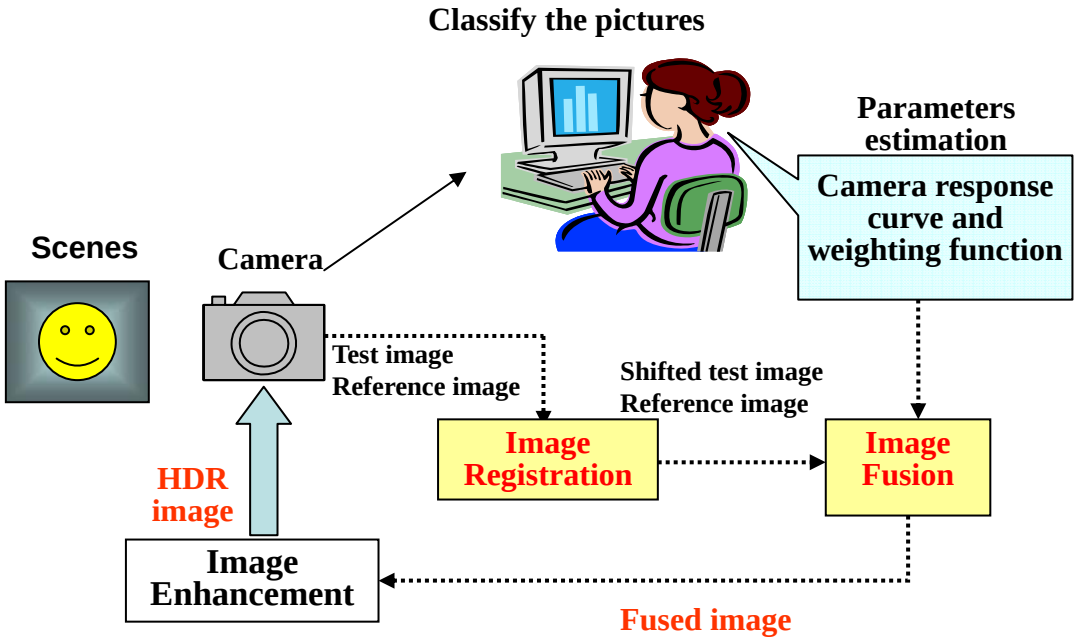

Fig. 5-1 Our experiment flow.

The examination flow is shown in **Fig. 5-2**. Using the "exposure bracket" mode can take three different exposed images continuously. The high exposed image is with bright object but saturated background. The low one is with real background but dim object. Image registration is our first operation in order to compensate the shifted value of object in low exposed image. The ADV comparison which will be described in section 5.2.1 is one of our examinations of Ward's and our proposed algorithms. After that, HDR image with bright object and real background is fused by our image fusion algorithm. The visual comparison of Wyckoff's and our proposed algorithms shown in section 5.2.2 is another examination.

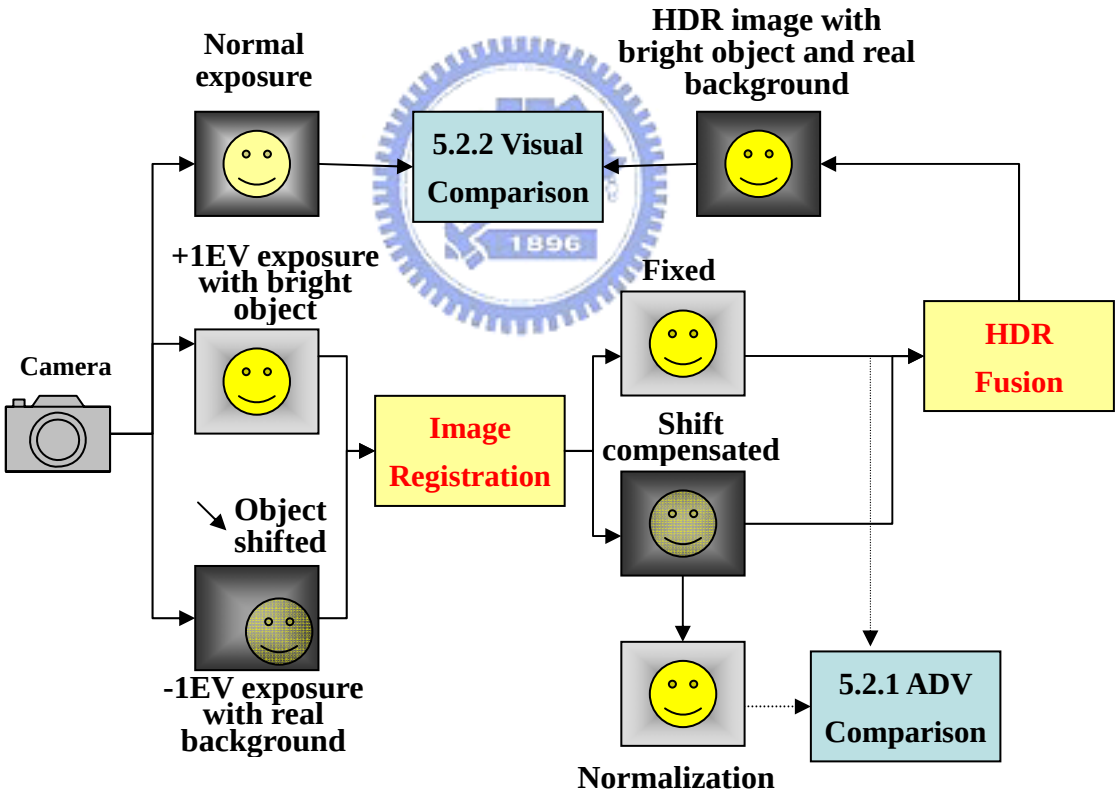

Fig. 5-2 Our examination flow.

5.2 Results

5.2.1 Image Registration

The “exposure bracket” mode makes it possible to practically simulate the real situation. Three different exposed images including +1EV, 0EV, and -1EV exposures are taken by the camera Nikon D70 without using tripod. Six sceneries shown in **Fig. 5-3** are chosen with near objects and far background.

(a) **(b)**

(c) **(d)**

(e) **(f)**

Fig. 5-3 (a)The CPT building with people. (b)The building shadow. (c)The person in front of a distant background. (d)The person in front of a complicated background. (e)The person inside the building. (f)The seaport with sunset.

For estimating absolute different values (ADV) of two images, a high exposed image was fixed and a low image was multiplied by four. Then the low exposed image was shifted by Ward's algorithm and our proposed algorithm respectively. Comparing ADV between each, the smaller ADV presents more accurate registration. ADV is defined by equation 5-1. Multiplication is required because of the exposure ratio. A comparison of ADV between Ward's algorithm and our proposed algorithm is listed in **Table 3-2**. The scenes of (a) to (f) are shown in **Fig. 5-3.**

$$ADV = \left(\left| R_{ref} - R_{shift} \cdot 4 \right| + \left| G_{ref} - G_{shift} \cdot 4 \right| + \left| B_{ref} - B_{shift} \cdot 4 \right| \right) / (3 * H * W) \quad (5\text{-}1)$$

Table 5-1 The comparison of ADV between Ward's algorithm and our proposed algorithm.

Scenes	Algorithms	
	Ward	Proposal
(a) Building(1)	89.254	69.76
(b) Building(2)	815.48	788.47
(c) Complicated background(1)	241.17	228.35
(d) Complicated background(2)	381.31	282.99
(e) Inside building	1363.30	1350.80
(f) Seaport with sunset	1109.60	1104.30

The above comparison shows that the ADV of our proposed algorithm is lower than Ward's algorithm. In other words, the accuracy of our proposed algorithm is higher than that of Ward's algorithm. In addition, our proposed algorithm can distinguish the difference between near and far scenes. For example, **Fig 5-4 (a)** and **(b)** are the two images combined

by low and high exposed images of Ward's and our proposed algorithm separately. The low exposed image is shifted and multiplied by four but high image is fixed. The near scenes, "color checkers," of Ward's and our proposed algorithm are shown in **Figs. 5-5 (a)** and **(b)** respectively. The far scenes, the building and the leaves, of Ward's algorithm and our proposed algorithm are shown in **Figs. 5-6 (a)** and **(b)**.

(a) **(b)**

Fig. 5-4 Two fused images with averaging. (a) Ward's algorithm and (b) our proposed algorithm.

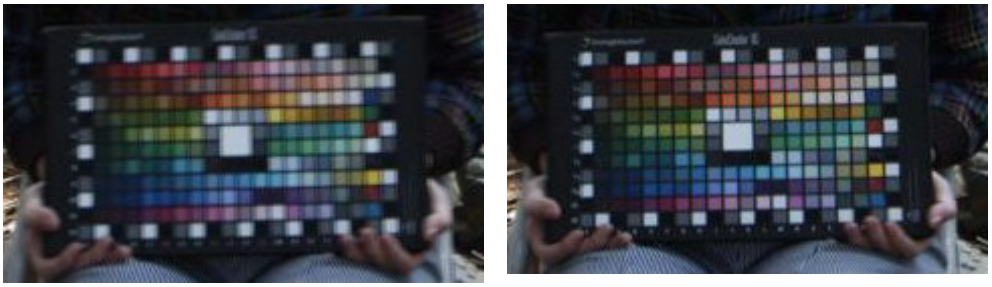

(a) **(b)**

Fig. 5-5 Two images of color checker which is the near scene. The shifted pixels in (a) is (-3,-1) from Ward's algorithm and in (b) is (-5,-1) from our proposed algorithm.

(a) **(b)**

Fig. 5-6 Two images of building and leaves which are the far scene. The shifted pixels in (a) is (-3,-1) from Ward's algorithm and in (b) is (0,-2) from our proposed algorithm.

Another example of image registration is shown in **Fig. 5-6. Figs. 6 (a) and (b)** are two images with high and low exposures respectively. The averaged images of Ward's algorithm and our proposed algorithm are shown in **Figs. 5-6 (c) and (d)** respectively. **Figs. 5-6 (e) and (f)** are each near scene. **Figs. 5-6 (g) and (h)** are each far scene.

(a) **(b)**

(c) **(d)**

(e)

(f)

(g)

(h)

Fig. 5-7 An example of image registration. (a) The fixed image with high exposure. (b) The shifted image with low exposure. (c)(d) The averaged images of Ward's and our proposed algorithms respectively. (e) The near scene of Ward's algorithm and the shifted pixels are (-6,1). (f) The near scene of our proposed algorithm and the shifted pixels are (-5,-1). (g) The far scene of Ward's algorithm and the shifted pixels are (-6,1). (h) The far scene of our proposed algorithm and the shifted pixels are (-7,-4).

In our proposed algorithm, the shifted pixels could be changed by objects with different distances, thus our averaged images are sharper than Ward's averaged images

5.2.2 HDR Fusion

(a) Parameters estimation:

The parameters, A and C, of this camera response curve are estimated by averaging parameters of six scenes. These parameters of six scenes are listed respectively in **Table 5-2**. Once the parameters were estimated, the response curve of our experimental camera is achieved which is shown in **Fig. 5-8**. The scenes of (a) to (f) are shown from **Fig. 5-9 to 5-14** respectively.

Table 5-2 The parameters, A and C, of six scenes.

Scenes	The parameters of camera response curve	
	A	C
(a) Strong backlight	15.60	0.062
(b) Seaport with sunset	23.05	0.042
(c) Building with shadow	4.94	0.194
(d) Library with shadow	11.75	0.086
(e) CPT building	6.55	0.152
(f) Inside building	11.61	0.084
Average	12.25	0.103

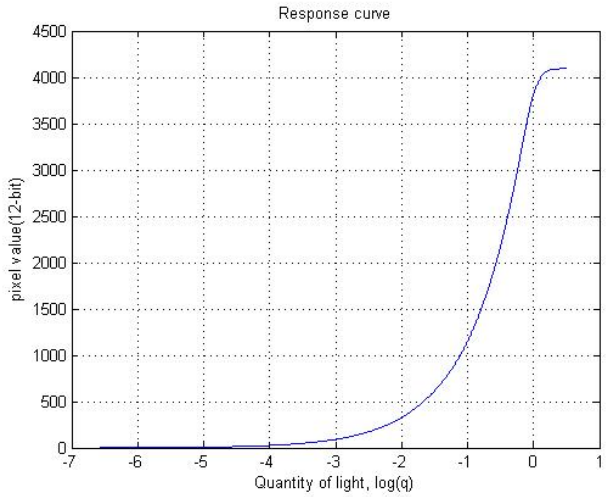

Fig. 5-8 The averaged response curve of experimental camera.

(b) Results:

We have already proposed novel image registration and fusion of HDR algorithms. The results are plotted from **Fig. 5-9 to 5-14**. The top two images of each figure are with high exposure (left) and low exposure (right). The second floor images of each figure are the comparison of the image with normal exposure (left) and the image of conventional fused HDR (right). The third floor images of each figure are the comparison of our registration image without registration (left) and with registration (right). The bottom images of each figure are the comparison of zoom-in images of our registration image without registration (left) and with registration (right). **Fig. 5-9** and **Fig. 5-10** are the scenes of the portrait in front of beautiful sky and sunset respectively. For our results, the portrait is clear and background is beautiful. **Fig. 5-11** and **Fig. 5-12** are the scenes with building shadow. For our results, the objects inside the shadow are bright and sky is unsaturated. **Fig. 5-13** is the scene with people in front of the building. For our results, the people and the trees are bright. **Fig. 5-14** is the scene with a portrait inside the building. For our results, the portrait is bright and outside sky is with cloud. In addition, all zoom-in images of our results with registration are sharper than that without registration.

(a)

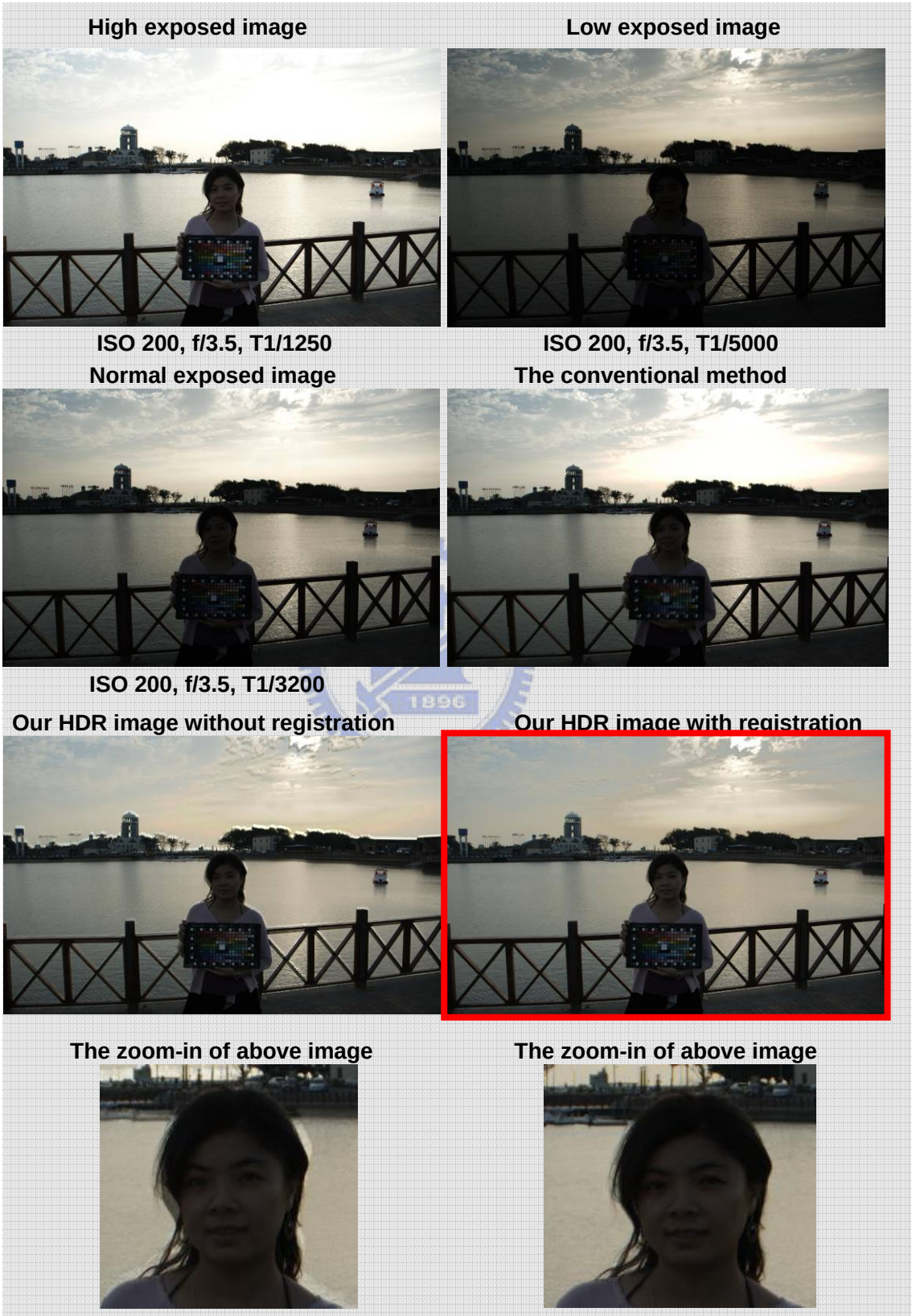

Fig. 5-9 The scenes of strong backlighting condition with beautiful sky.

(b)

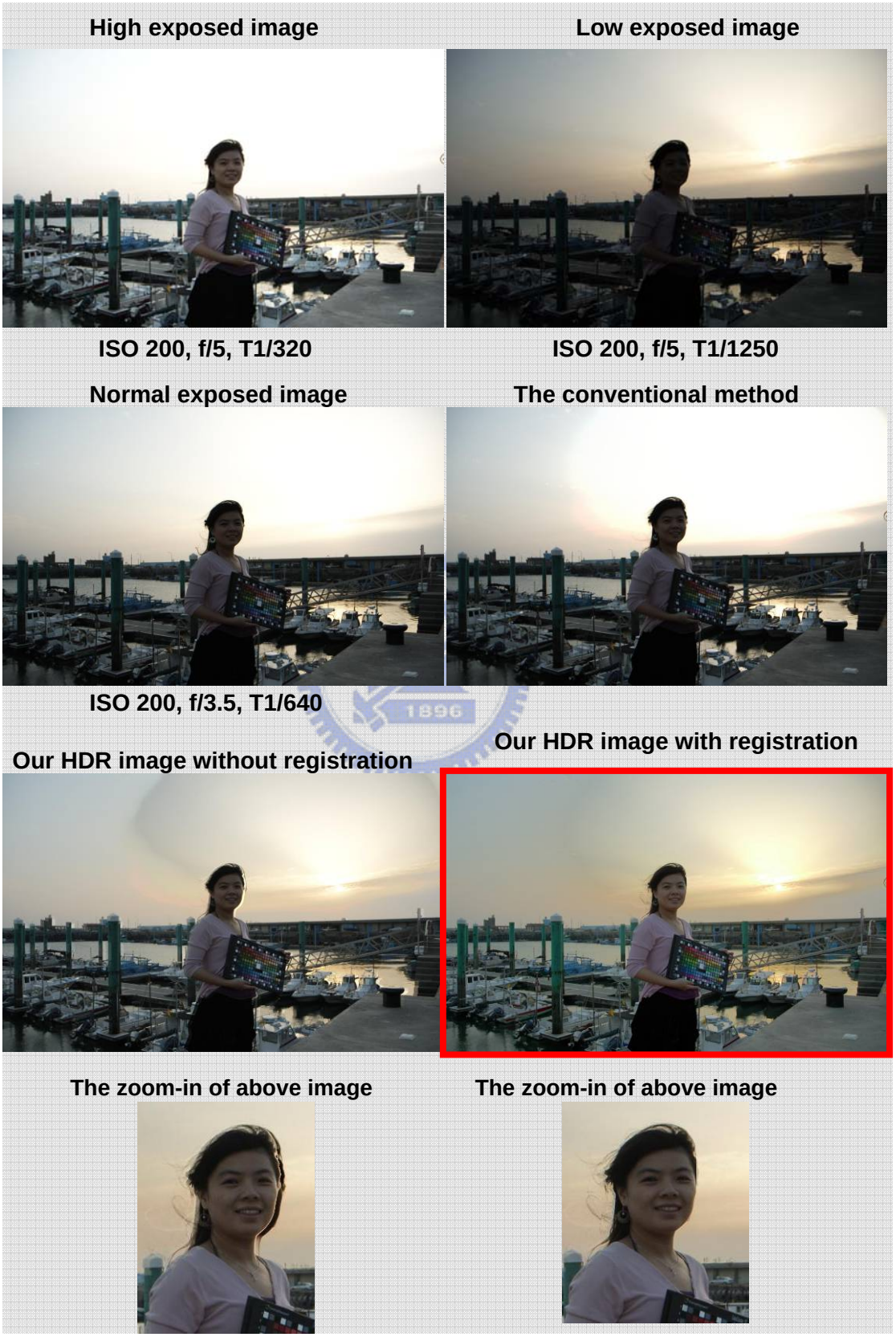

Fig. 5-10 The scenes of strong backlighting condition with beautiful sunset.

(c)

Fig. 5-11 The scenes of the backlighting condition with building shadow.

(d)

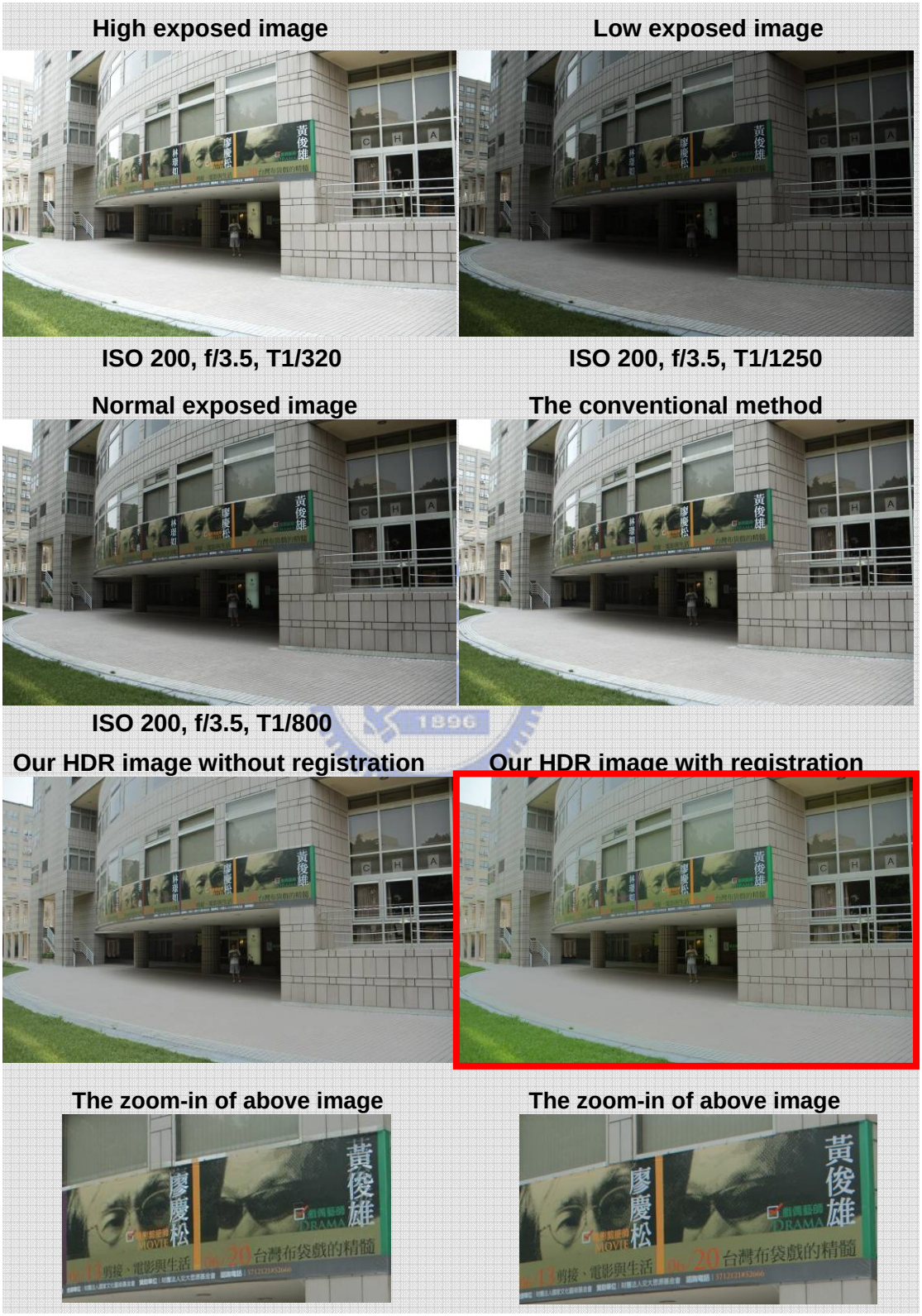

Fig. 5-12 The scenes of the backlighting condition with building shadow.

(e)

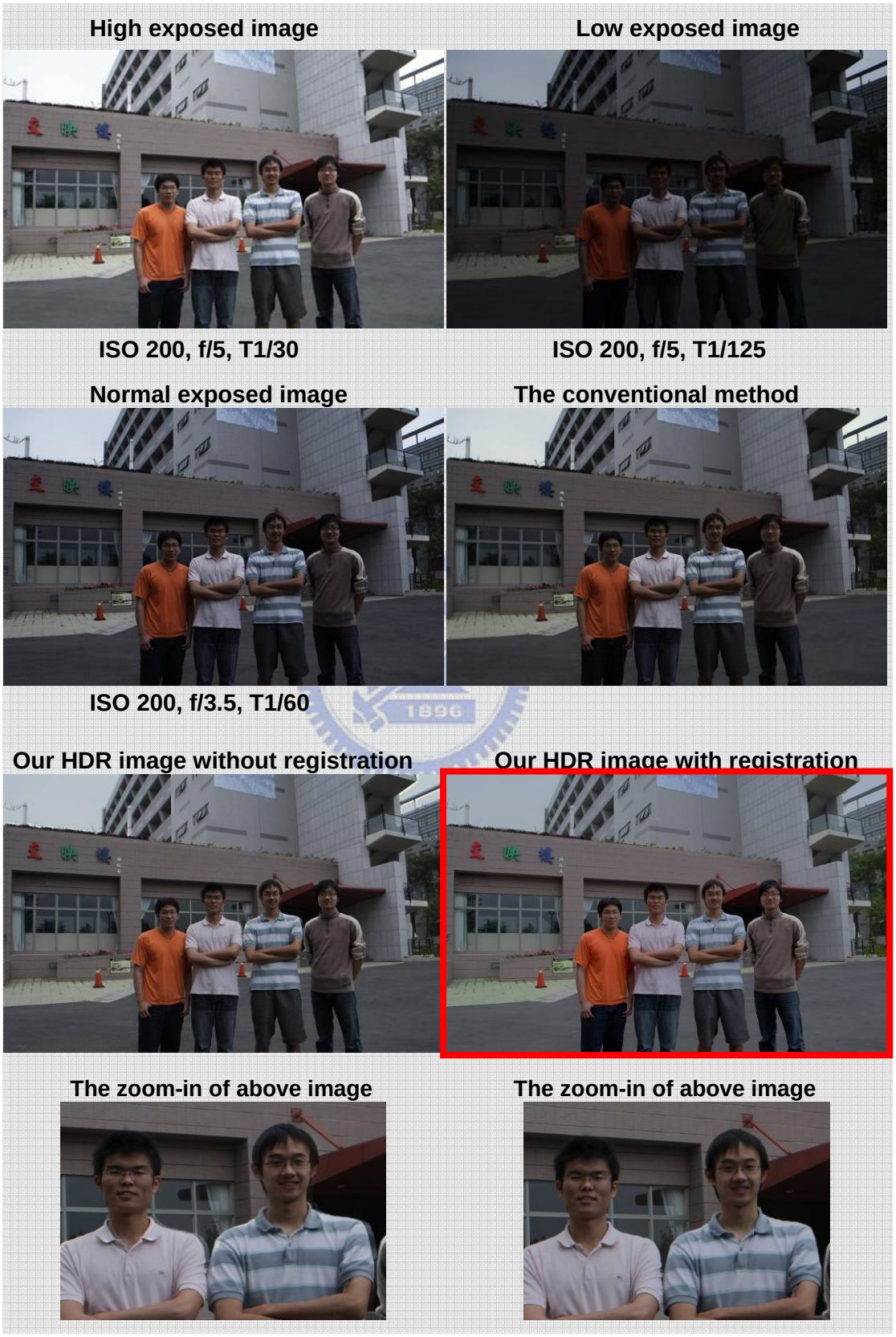

Fig. 5-13 The scenes of the near people in front of building.

(f)

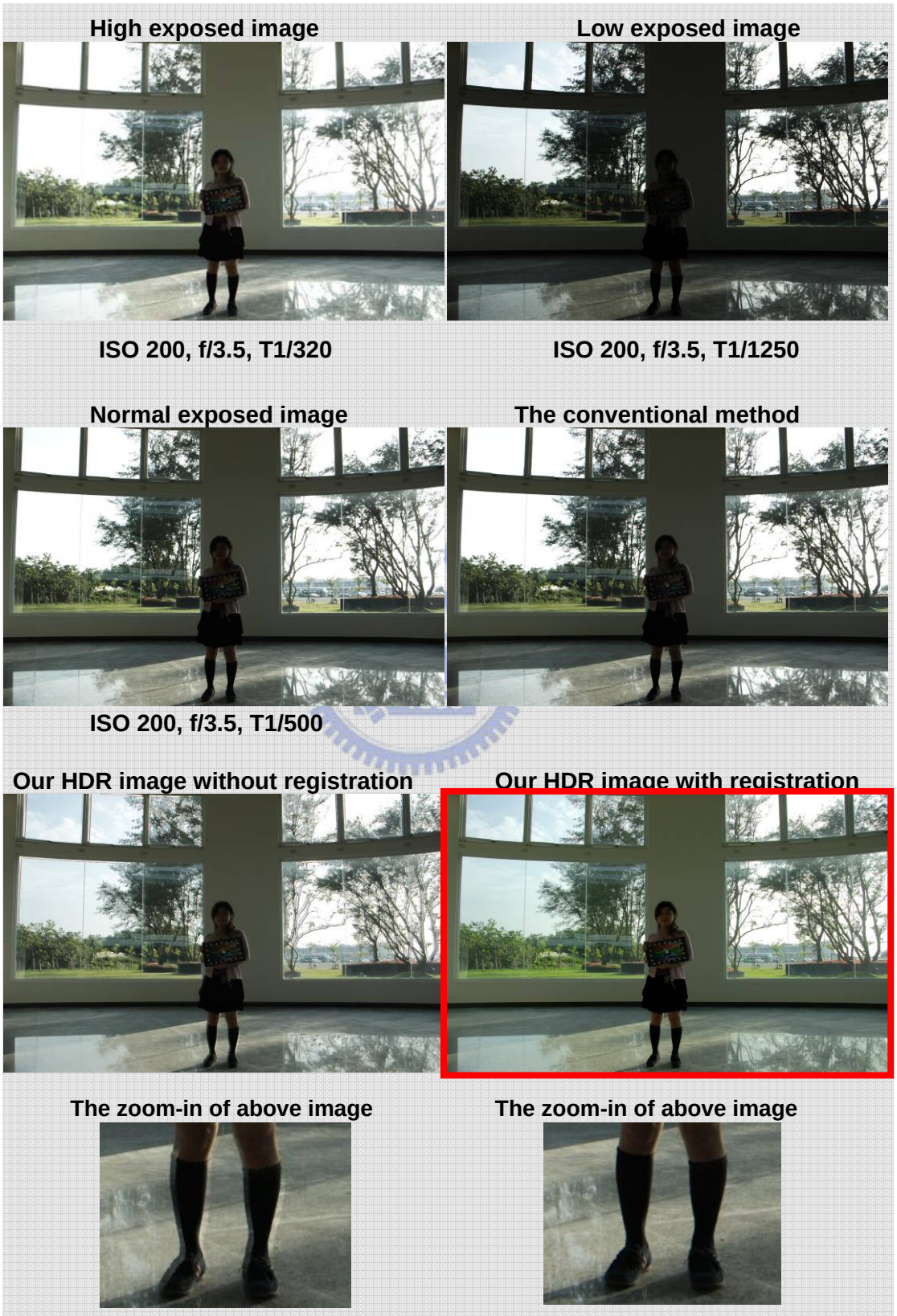

Fig. 5-14 The scenes of the portrait inside the building.

5.3 Summary

According to the proposed image registration and fusion for HDR algorithms, we have setup our examination flow and experiment flow respectively. For image registration technique, the issues of Ward's algorithm were improved especially the issue of near and far scenes. Due to the examined result of the absolute different value (ADV), the smaller ADV of our algorithm demonstrates that the accuracy can be higher and the issue of near and far scenes can be improved by our proposed algorithm.

For the fusion application of HDR, the performance of our fused HDR image was improved especially in the scenes with bright and dim luminance. In addition, the sharper edge of our result could be demonstrated that the image registration technique is required. As a result, our proposed registration and fusion algorithms are reliable because of the improved performance of our HDR images.